

## Session: Secondary and Finishing Operations

### Influence of process parameters and alloying type on properties of laser quenched P/M-steels

E. Colombini<sup>1</sup>, G.F. Bocchini<sup>2</sup>, G.Parigi<sup>3</sup>, R. Sola<sup>1</sup>, P.Veronesi<sup>1</sup>, G. Poli<sup>1</sup>

1 Department of Engineering "Enzo Ferrari", University of Modena and Reggio Emilia, Via Vignolese 905/A- 41125 Modena, Italy

2 P/M Consultant, Rapallo, Italy

3 STAV S.r.l., Via della Lora, 18, Barberino di Mugello, Firenze, Italy

#### Abstract

Different alloyed P/M steels have been laser quenched in industrial equipment laser diodes (4 kW, controlled by material surface temperature). The aim of this work is to investigate their responses to different process condition and different alloying metals, i.e. Cu, Ni, Mo, Cr and C. Furthermore the microstructure of hardened layer, heat affected zone (HAZ) and bulk zone Pre-alloyed, diffusion bonded and hybrid raw materials have been used. Design of Experiments has been the approach for evaluating the effect of treatment parameters (i.e temperature, spot size and speed) and to develop predictive models, correlating such parameters to hardening depth and scratch hardness number. Results demonstrated which valuable properties could be achieved, even through relatively low alloying. The promising results are encouraging since they allow to forecast a possible positive combination of high local hardness and wear resistance of high precision P/M part.

#### Introduction

Laser transformation hardening [LHT] competes with many established methods of surface treatment. [1-2]. LTH [3] involves the use of laser as a heat source. When a laser beam impinges on a surface, part of its energy is absorbed as heat at the surface. If the power density of the laser beam is sufficiently high, heat will be generated at the surface, at a rate higher than heat conduction to the interior can remove it, and the temperature in the surface layer will increase rapidly. In a very short time, a thin surface layer will reach the austenitizing temperatures. This area is subsequently cooled rapidly down by heat conduction to the interior after the beam has passed, forming fine martensite structure. Therefore, treatment temperature is usually established to give peak temperatures well above those employed in conventional hardening, to ensure austenitization and carbon homogenization, but not high enough to initiate surface melting. Critical factors in LTH are obtaining adequate amount of austenite with appropriate carbon content during heating, considering the high heating rate, and avoiding surface melting [1]. More, the hold time above  $A_{c3}$  line must be sufficient to form homogeneous austenite and to distribute homogeneously carbon. By selecting the correct power density and speed of the laser spot, the material will harden to the desired depth. [4]

The laser hardening has been performed by 4 kW laser diode, driven by a anthropomorphic robot, to process the surface layers of samples. An optical pyrometer, positioned on the laser head, integrated by means of dichroic glass, controls the laser source by measuring the surface temperature of the exposed material. The laser control system automatically changes the emitted power, to achieve the desired temperature in the processing zone. This feature is particularly useful because for small samples, as laser exposure proceeds, the average sample temperature increases with time. This requires a feedback control on the laser source power, to avoid overheating. The list below indicates the typical ranges of operating parameters of the equipment:

- Temperature (T) (range 1150-1350 °C)
- Focal length (f length) (range 150-250 mm),
- Laser beam speed (v) (range 2-10 mm/s),

- Spot size (range 3-7 mm x mm).

## Experimental Procedures

Table I lists the six different materials (Table I) investigated and the reference one, named SH, obtained by sinter-hardening followed by stress relieving, which stands for the current state. Laser trail has been performed on actual component (A, B, M, N, O), as shown in Figure 1, and on block material C. To study the effect of process parameters, each component has been manufactured by 8 different processing sets, as shown in Table II. Only one set of parameters has been applied to harden the parts A and B. In this study, among laser parameters only speed and temperature have been varied. Spot size and focal length have been kept constant: respectively 7x7 [mm x mm] and 250 [mm].

Table I: Chemical composition of investigated materials

Code	Base material	C %	Cr %	Cu %	Mo %	Ni %
A	Prealloyed powder (Astaloy Mo, from Höganäs AB)	0.7	-	2.0	1.5	-
B	Prealloyed powder (Astaloy CrA, from Höganäs AB)	0.7	1.8	1.0	-	-
C	Prealloyed powder (Astaloy CrM, from Höganäs AB)	0.5	3.0	-	0.5	-
M	Prealloyed powder (Astaloy CrL, from Höganäs AB)	0.7	1.8			
N	Mixed powder	0.7		2		
O	Diffusion-bonded powder (Distaloy AB, from Höganäs AB)	0.6	-	1.5	0.5	1.75
SH	Prealloyed powder (Astaloy CrM, from Höganäs AB)	0.5	3.0		0.5	

Table II: Laser hardening parameters applied to laser hardening of samples shown Table I

Sample	Surface T	Speed v	Sample	Surface T	Speed v
	[°C]	[mm/s]		[°C]	[mm/s]
C1	1200	2	C5	1250	6
C2	1200	4	C6	1300	6
C3	1200	6	C7	1150	6
C4	1200	8	C8	1200	10
M1	1200	2	M5	1250	6
M2	1200	4	M6	1300	6
M3	1200	6	M7	1150	6
M4	1200	8	M8	1200	10
N1	1200	2	N5	1250	6
N2	1200	4	N6	1300	6
N3	1200	6	N7	1150	6
N4	1200	8	N8	1200	10
A	1200	8	B	1200	8

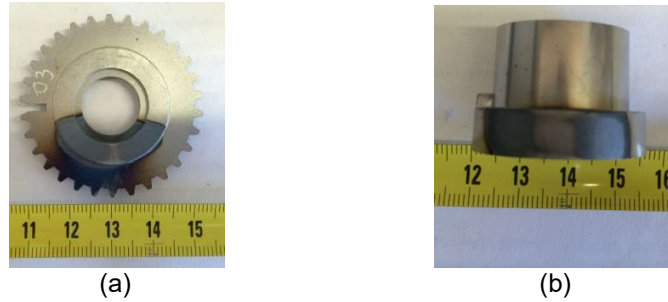


Fig. 1: An example of treated components, (a) sample O, (b) sample M

The following sample characterizations have been performed:

- Energy Density.
- Surface hardness, HV0.5, (500 g load) MicroconsultPMV - 1000TM.
- Hardness depth, evaluated by HV0.1 hardness profile on sample section, The hardening depth is taken as the distance from the surface for which the hardness profile intersects the average hardness value measured in the core of sample. Hardness HV0.1 Vickers has been measured by Wolpert W Group Micro-Vickers hardness Tester 402 MVD (100 g for 15 s). [6]
- Geometric parameters (depth and width) of laser hardening zone, measured by Stereographic microscope Olympus SZX 10 on a cross section, only in sample C, because in the other components trail shape depends on real part geometry.
- Scratch Hardness Number (SHN), evaluated according to ASTM G171-03 by CSM. Open Platform instrument: Rockwell indenter, 200  $\mu\text{m}$  radius diamond tip, 4 mm scratch length; 2 mm/min scratch speed, 3 N normal force, 3 scratches for each sample, measures each 100  $\mu\text{m}$  to obtain a profile.

Cross-sections for microscopy observations have been obtained by grinding (Labotom 3- Struers), afterwards samples have been resin-mounted, by Citopress 1 and subjected to polishing (up to polishing cloths 1  $\mu\text{m}$ , by Labopol 5- Struers). Etching, for revealing the microstructure, has been performed by full immersion of the samples in 2% Nital solution, for 20 s. Metallographic observation has been performed by Optical Microscope GX51 (Camera SC30). Samples are identified according to the codes listed in Table II.

## Experimental Results

As above stated, laser heat treatment is a localized heat treatment process involving only heating, with relatively low values of energy density (to avoid surface melting). The energy density (ED) [12] of the radiation may be varied by defocusing the beam, i.e., through a displacement of the irradiated surface by a certain distance from the focal plane of the laser objective lens. The calculation of energy density is based on the Eq. (1):

$$ED = \frac{P}{DV} \quad (1)$$

where P is the laser beam power, D is the spot-diameter and v is the travel speed of the beam. [7] Figure 2 shows the effect of T [ $^{\circ}\text{C}$ ] and laser beam speed [mm/min] on energy density [ $\text{J}/\text{cm}^2$ ], In detail for high speed and high temperature the energy density reaches the minimum value. Figure 3 shows the effect the laser beam speed and temperature on laser track dimension, in terms of track depth, measured by optical microscopy. High temperature leads to high laser trail depth, while the speed is poorly affecting track depth. This can be ascribed to the control system of the laser head, which adjusts the laser power to

reach the set temperature level. Hence, despite the imposed variation of speed, power is adjusted to match the set point temperature and speed becomes a less relevant parameter.

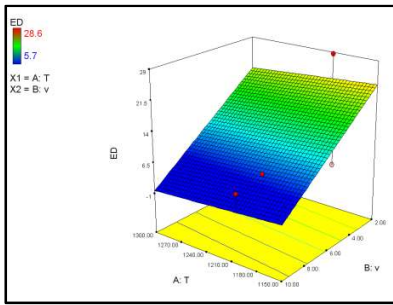


Fig. 2. Influence of laser speed and surface temperature on the energy density

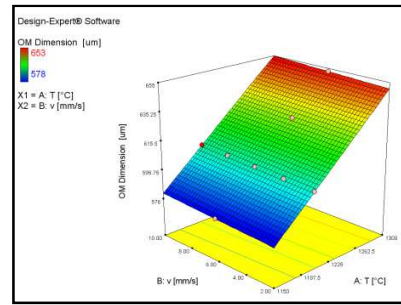


Fig. 3. Effect the laser beam speed and temperature on laser track dimension

ANOVA analyses, to correlate surface hardness (HV0.5), temperature and speed, indicates a not-significant relationship.

Figure 4 shows the effect of different process parameters and materials on the measured hardening depth. Hence, to better define the hardening depth a further set of measurements, using the Scratch Hardness Number, has been performed. Figures 5 and 6 show the results.

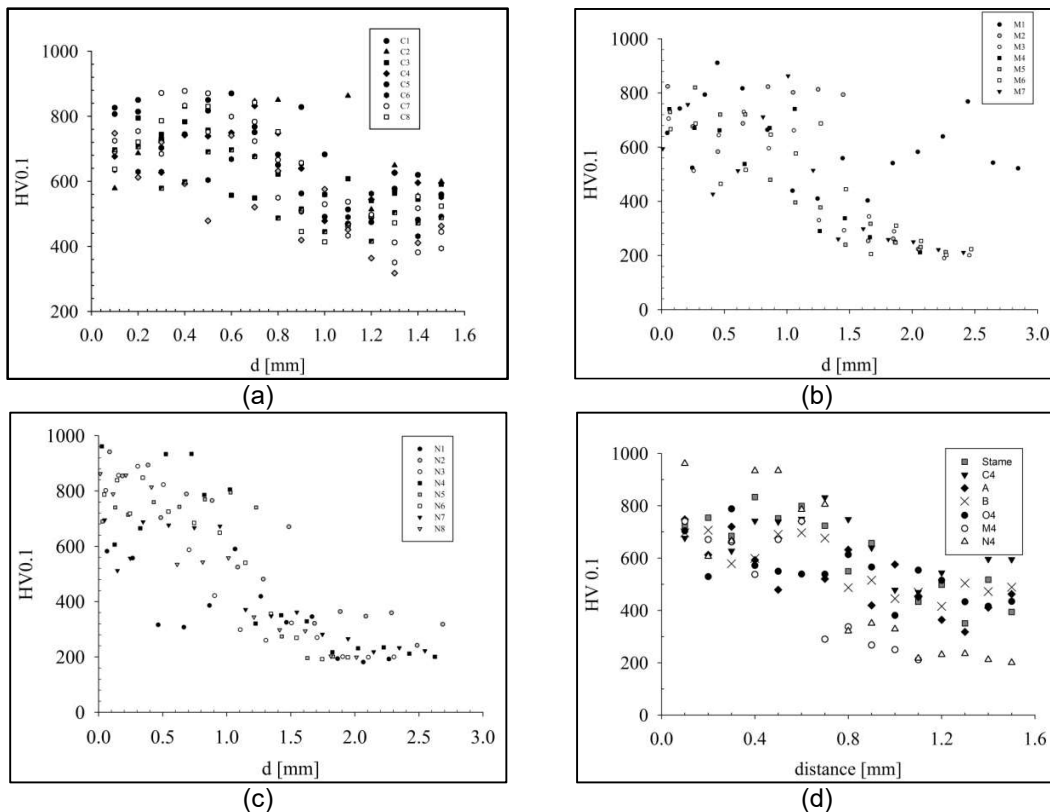


Fig. 4: Profile hardness of samples based on the same material, but with different process parameters. In detail: (a) sample C, (b) sample M, (c) sample N. Fig. 4 (d) shows the indentation profile of samples obtained by different materials but treated by the same process parameter.

Samples M and N show a higher penetration depth than sample C: respectively 1.4 mm, 1.5 mm and 1 mm. The variation of process parameters do not lead to strong differences among the penetration depths. Evaluated according to ASTM G171-03, Scratch Hardness Number (SHN) is a measure of the scratch resistance of a surface. On surface hardened samples, it is expected that the width of the track reflects the micro-hardness profiles, with larger SHN in correspondence of maximum hardness. However, the type of indenter and the mode of load application during SHN measurements, differs from the microhardness measurements, hence a direct correlation is not always possible.

SHN have been evaluated on selected samples, in details C4, A, B and C6 and C8. Sample C4 presents the highest SHN, maintained for few tenths of mm from the surface (point 0 on x-axis), despite the relatively low hardening temperature and high processing speed used for this sample. This behavior could be due to the higher cooling rates achievable under these conditions. The remaining samples confirm the expected trend of having higher SHN near the surface, then progressively decreasing in the bulk of the material. Rather interestingly, the maximum SHN is not on the surface, but some micrometers below it, in agreement with literature results. [12]

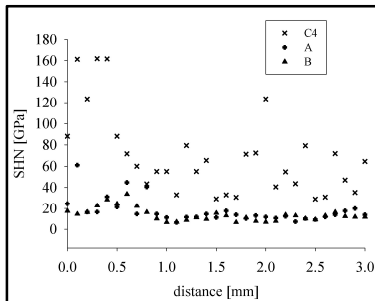


Fig. 5. SHN samples obtained from different alloys but applying the same process parameters

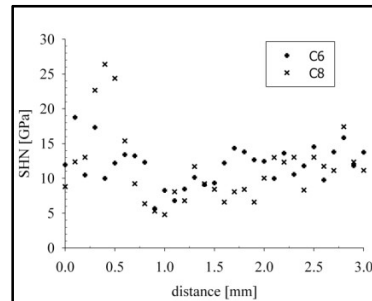


Fig. 6. SHN samples obtained from the same alloy but applying different process parameters

Figure 7 shows the sample microstructure of laser heat-treated zone, observed by optical microscope.



Fig. 7. OM of laser trail cross section

By means of SEM/EDS analysis it is possible to observe some carbon loss in the laser treated zone (Fig. 8 (a)), with very fine martensitic microstructure (Figure 8 (a)), and bainite, (Figure 8 (c)) in the transition zone. As expected, the bulk is not affected by laser hardening process (Fig. 8 (d)).

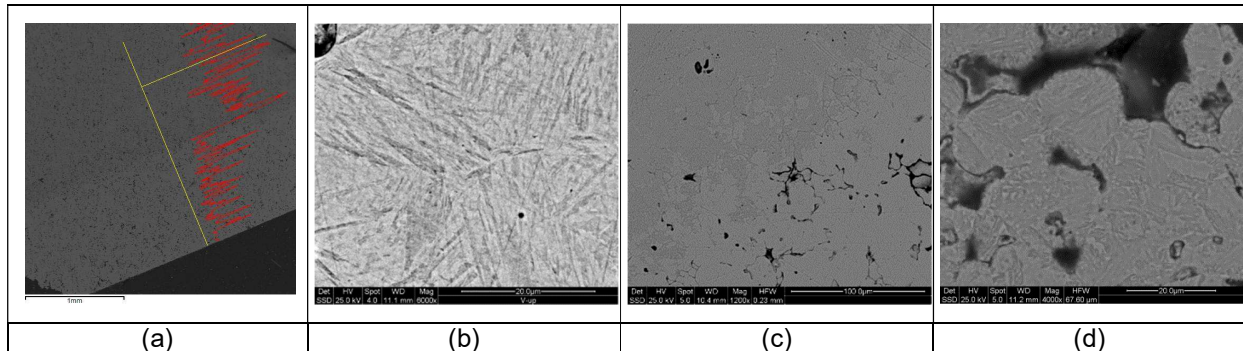


Figure 8. (a) EDS analysis to highlight the decarburization, (b) hardness layer, (c) transition zone, (d) bulk zone microstructure

## Conclusion

This work reveals the possibility to apply a selective and precise hardening treatment, like Laser Transformation hardening (LHT), to P/M steel parts. The tests were performed both on reference block and on real components, to prove the process feasibility.

Thanks to ANOVA analysis, the correlation between energy density (ED) and optical dimension of treated zone has been identified. By increasing temperature and speed, the ED decreases, indeed at high temperature and speed the heated zone is larger. At the same speed, a temperature increase leads to a decrease of surface hardness. The study enable to reveal the main effect on laser process between process parameter and on differently alloyed PM steels The hardness depth is more depending on the different of materials than on the change of process parameters. Scratch tests double check the results. The sample C shows a parabolic profile of the hardened zone, from the surface to the bulk the hardened zone, where the central part corresponds to the focusing point of laser. Microstructures of all samples present very fine martensitic structure on the top of laser trail, and bainite microstructure on transition zone, as literature related . Moreover The transition zone between the laser affected zone and the base metal exhibits a micro hardness gradient. By comparison among LHT specimens and sinter-hardened and stress-relieved one, (similar chemical compositions) penetration depth and hardness values appear similar.

## References

1. D. Rodziňák, J. Čerňan, R. Zahradníček, Effect of Laser Hardening on the Properties of PM Steels, *Acta Metallurgica Slovaca*, Kosice, (2013), 19 (4), pp. 282-291
2. S. Santhanakrishnan, N. B. Dahotre, Laser Surface Hardening, in *ASM Handbook, Steel Heat Treating Fundamentals and Processes*, J. Dossett and G. E. Totten, editors, ASM (2013), 4A
3. R. Rowshan, Process Control during Laser Transformation Hardening, PhD Thesis, Miskolc University. Miskolc, Hungaria, 2007
4. O. Sandven, Laser Surface Transformation Hardening, *Surface Engineering, Metals Handbook*, ASM 9th Ed., Vol. 4, pp. 507-517
5. E. Mosca, M. Lampugnani, Hardness and Microhardness Test on PM Materials, *Metal Powder Report*, (1984), pp. 148-150
6. P. D. Babu, G. Buvanashakaran, K. R. Balasubrama, Experimental studies on the microstructures and hardness of laser transformation hardening of alloy steel, *Transactions of the Canadian Society for Mechanical Engineering* Vol. 36, No. 3, 2012, pp 241-258